ELSEVIER

Journal of Non-Crystalline Solids 299–302 (2002) 1213–1218

JOURNAL OF NON-CRYSTALLINE SOLIDS

www.elsevier.com/locate/jnoncrysol

Study of a-SiGe:H films and n–i–p devices used in high efficiency triple junction solar cells

Pratima Agarwal [a,b,*], H. Povolny [a], S. Han [a], X. Deng [a]

[a] Department of Physics and Astronomy, University of Toledo, Toledo, OH 43606, USA
[b] Department of Physics, Indian Institute of Technology Guwahati, North Guwahati, Guwahati 781 039, India

Abstract

We report our systematic studies on a-SiGe:H thin films and n–i–p solar cells for GeH_4/Si_2H_6 ratio varying from 1.43 to 0. This results in a variation of band gap from 1.37 to 1.84 eV. The FTIR studies show that the total hydrogen content in these films decreases as Ge content increases. For Ge rich films, the hydrogen also goes in to Ge–H mode. *I–V* measurements on n–i–p solar cells with i-layer having different Ge content show that as Ge content increase, Short circuit current (J_{sc}) increases, whereas open circuit voltage (V_{oc}), fill factor (FF) and conversion efficiency (η) decrease. For Ge rich films, J_{sc} does not significantly increase after GeH_4/Si_2H_6 ratio increases beyond 0.72; however V_{oc}, FF and η decrease drastically. The quantum efficiency (QE) measurements in the subgap absorption range show that band gap and Urbach slope of the i-layer can very well be estimated in the devices. © 2002 Elsevier Science B.V. All rights reserved.

PACS: 63.50; 71.23.Cq; 71.55.Jr; 78.30.Ly; 81.15.Gh; 84.60.Jt

1. Introduction

Amorphous silicon germanium alloys are used as i-layers in multi-junction amorphous silicon based solar cells [1]. The advantage is that by varying the amount of Ge in the i-layer, the band gap can be varied from ~1.1 eV (in pure a-Ge:H films) to ~1.8 eV (pure a-Si:H films). This allows the capture of the full range of the solar spectra in different layers and thus increases the efficiency of the solar cells if process parameters, such that band gap and thickness are properly adjusted. The efficiency and stability of solar cells depends upon the properties and stability of the component i-layers. It is, thus, necessary to study the single layers and corresponding devices to improve the device quality.

In this paper, we report our studies on a series of a-SiGe:H single layers and n–i–p solar cells with varying $[GeH_4]/[Si_2H_6]$ ratio. Study of a-SiGe:H is not new and quite a few reports are available in literature. However, the present study is different in the following way: some of the a-SiGe single layers and cells have the $[GeH_4]/[Si_2H_6]$ ratio and other deposition parameters corresponding to the top, middle and bottom cells presently used in our triple junction solar cells with 11% efficiency [2]. In addition, cells with intermediate and higher $[GeH_4]/[Si_2H_6]$ ratio are also made for the purpose

* Corresponding author.
E-mail addresses: pratima@iitg.ernet.in, apratima@post-mark.net (P. Agarwal).

0022-3093/02/$ - see front matter © 2002 Elsevier Science B.V. All rights reserved.
PII: S0022-3093(01)01141-3

of comparison and complete systematic study. The motivation of this study is to (1) demonstrate the performance of the component cells used in our standard triple junction solar cells and (2) to find out whether a different Ge content in the bottom or middle cell would be more suitable for the triple cell.

2. Experimental details

a-SiGe:H films, approximately 0.7 μm thick, are deposited on Corning 7059 glass, c-Si substrates and stainless steel (SS) with varying GeH_4 to Si_2H_6 ratio. Table 1 shows the deposition conditions for these a-SiGe:H films, including the $[GeH_4]/[Si_2H_6]$, H_2 flow and the substrate temperature. It is to be noted that GD357, GD359 and GD361 are corresponding to the i-layers in our regular bottom, middle and top cells [2]. These samples serve as the reference points for this set of samples. Transmission measurements in the Vis–NIR range are done to determine the thickness, optical gap and refractive index of these films [3]. The FTIR measurements are also done on films deposited on crystalline silicon substrates in the range of 400–4000 cm^{-1} to determine the different Si–H and Ge–H bonding modes and to estimate the total amount of hydrogen present in these films [4].

n–i–p solar cells using these a-SiGe:H materials as the i-layers are deposited on SS as well as on substrate with back reflector. The device structure is SS (BR)/a-Si n^+/n–i buffer/a-SiGe:H (a-Si:H) absorber layer/i–p buffer/μc-Sip^+/ITO. The n–i and i–p buffer layers consist of a-Si:H buffer layers next to the doped layers and absorber layer. Unlike our normal cells, these buffer layers do not have any graded band gap [5]. The SiGe absorber layer is also prepared without any germanium grading to match these with the corresponding single layer films. *I–V* measurements are taken under a Xe lamp solar simulator. Quantum efficiency (QE) measurements are done in the range of 420–900 nm using tungsten lamp. Light soaking is done under AM1 light from a metal halide lamp for 1000 h and the performance of these cells is measured at different stages of light soaking. The QE measurements are also done in the subgap absorption range to estimate the band gap and Urbach tail slope of the absorber i-layer in the device.

3. Results and discussion

3.1. Single layer amorphous silicon germanium films

Table 1 lists the band gap of a-SiGe:H films as determined by transmission measurements [3] along with the deposition conditions such as the $[GeH_4]/[Si_2H_6]$ ratio, hydrogen dilution ($R = \{[GeH_4] + [Si_2H_6]\}/[H_2]$), substrate temperature. The band gap decreases from 1.84 to 1.37 eV as $[GeH_4]/[Si_2H_6]$ ratio increases from 0 to 1.43. To find out the H content and its bonding configuration in our films, infrared absorption for these films is measured using an FTIR spectroscopy in the range of 400–4000 cm^{-1}.

Figs. 1 and 2 show the absorption spectrum of these a-SiGe:H films in the 400–850 and 1800–2200 cm^{-1} ranges corresponding to Si–H wagging and stretching modes. The crystalline silicon sub-

Table 1
Deposition conditions, band gap, hydrogen concentration and the ratio of hydrogen in different modes for single layer a-SiGe:H thin films

Sample number	$[GeH_4]/[Si_2H_6]$	R	T_s (°C)	E_g (eV)	[H]Ge (at.%)	[H]Si (at.%)	$[SiH_2]/[SiH]$	$[GeH]/[SiH]$	$[GeH_2]/[GeH]$
GD361	0.00	32	200	1.84	0.055	16.4	0.229		
GD360	0.18	33	250	1.72	1.237	16.31	0.281	0.044	0.132
GD359	0.36	33	300	1.65	1.348	12.98	0.267	0.072	0.191
GD358	0.50	33	350	1.57	1.167	9.73	0.097	0.076	0.139
GD357	0.72	35	400	1.50	1.421	8.39	0.083	0.192	0.231
GD430	1.00	42	400	1.43	1.811	5.21			
GD431	1.43	50	400	1.37	2.077	5.59			

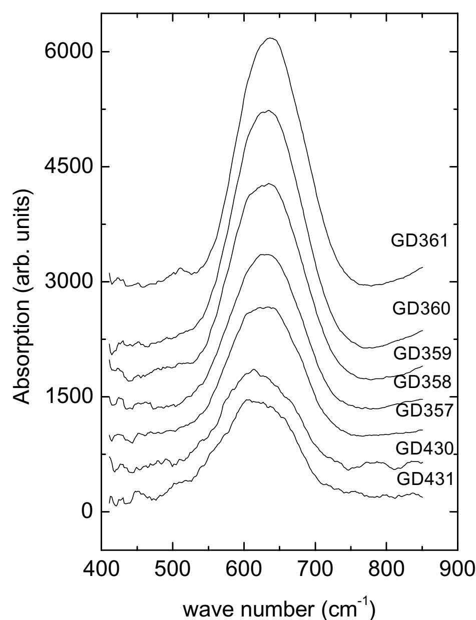

Fig. 1. FTIR absorption spectra for a-SiGe:H films in 400–850 cm^{-1} range. The curves have been shifted vertically for clarity.

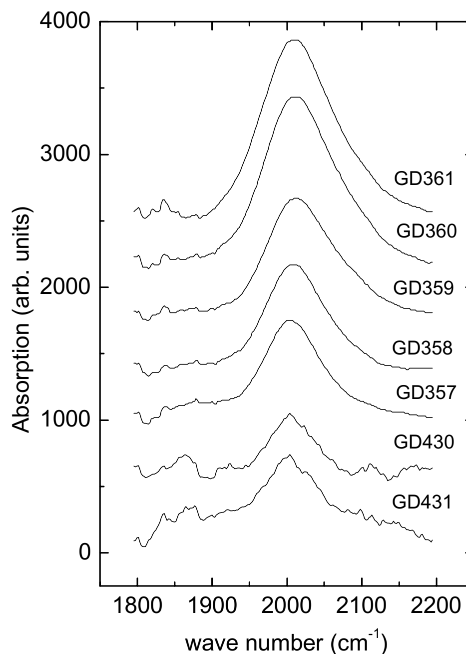

Fig. 2. FTIR absorption spectra for a-SiGe:H films in 1800–2200 cm^{-1} range. The curves have been shifted vertically for clarity.

strate from the same lot has been used to determine the baseline for these measurements. The curves in these figures are shifted vertically for clarity. The FTIR spectrum in 400–850 cm^{-1} range is de-convoluted into two peaks at 570 and 637 cm^{-1} corresponding to Ge–H and Si–H wagging modes, respectively. The area under each curve is then used to calculate the amount of hydrogen bonded with Ge and Si [4]. This is also listed in Table 1. The total amount of hydrogen in these films decreases as [Ge] content increases in these films as reported in literature as well [6]. Further more hydrogen goes into the Ge–H mode in Ge rich films. A higher deposition temperature and lower dilution could be a possible cause for less hydrogen in Ge rich films.

The FTIR spectrum in 1800–2200 cm^{-1} range is also de-convoluted into four peaks at 1877, 1980, 2007 and 2087 cm^{-1} corresponding to Ge–H, Ge–H_2, Si–H and Si–H_2 stretching modes. The area under these peaks is then used to determine the [Si–H_2]/[Si–H], [Ge–H_2]/[Ge–H] and [Ge–H]/[Si–H] ratio. In accordance with the spectrum near 400–850 cm^{-1}, [Ge–H]/[Si–H] ratio increases as Ge content increases. Further, for a-Si:H films prepared without any [Si–H_2]/[Si–H] ratio is about 0.23, which increases to about 0.27 for films with intermediate [Ge]. In Ge rich films, the ratio decreases to 0.09. This could be due to the fact that in Ge rich films a large part of total hydrogen is bonded in Ge–H and Ge–H_2 form. Further, Ge rich films are deposited at higher temperature, which will prevent the formation of Si–H_2 bonds in these films. Hedegus et al. [7] also reported a decrease in dihydride with increasing deposition temperature.

3.2. Amorphous silicon germanium n–i–p devices

Single junction n–i–p devices corresponding to the i-layers discussed above are fabricated on SS substrates and were characterized for their performance under AM1 light from a Xenon lamp solar simulator. Table 2 lists the V_{oc}, J_{sc}, fill factor (FF), conversion efficiency (η) for these cells. It is to be noted that in this case, Ge rich samples were not prepared with graded buffer layer and absorber layers, unlike our standard bottom cells [5].

Table 2
Deposition conditions and cell parameters for n–i–p solar cells

Sample number	Cell	$[GeH_4]/[Si_2H_6]$	d (nm)	V_{oc} (V)	J_{sc} (mA/cm^2)	FF (%)	η ($\% \pm 0.2$)	J_{ph} (mA/cm^2)	% change in η	E_g ($eV \pm 0.01$)	E_0 ($meV \pm 2$)
GD441		1.43	151	0.519	17.9	43.1	5.04	14.21	10 ± 1		
GD442		1.00	184	0.577	18.2	50.1	5.25	14.75	9 ± 1	1.44	37
GD443	Bot	0.72	171	0.660	17.4	55.3	6.36	13.63	21 ± 2		
GD435	Bot	0.72	153	0.666	19.1	54.3	6.91	13.43	16 ± 2	1.48	40
GD436		0.50	171	0.744	14.1	63.9	6.72	12.22	10 ± 1	1.60	38
GD437	Mid	0.36	209	0.810	16.1	61.8	8.05	11.58	6 ± 1[a]	1.67	40
GD438		0.18	215	0.849	12.0	63.1	6.44	9.73	17 ± 2	1.73	41
GD439	Top	0.00	194	0.895	10.3	69.5	6.40	8.12	3 ± 1	1.83	49

[a] After 10 h of light soaking.

The parameter values are comparable to our standard cells. A slight decrease in maximum power may be due to the band gap discontinuity at the interface of these low band gap cells. We observe that J_{sc} increases, whereas V_{oc}, FF and η of solar cells decreases with increasing Ge content. It is further observed that J_{sc} does not increase significantly, whereas a drastic decrease in V_{oc}, FF and η is observed when $[GeH_4]/[Si_2H_6]$ is increased beyond 0.72. The lack of further increase in J_{sc} with increasing Ge content is due to lower collection of carriers when the i-layer material quality is poor.

The spectral responses of devices in this set were measured in the 400–1000 nm range. The monochromatic light beam is focused inside the cell. Therefore, the measurement is independent of the variation in the cell area. The integrated current density (J_{ph}) values calculated using QE and normalized AM1.5 global (NAM1.5Gl) solar ir-radiance, gives us the estimate of the short circuit current under that solar spectra and are listed in Table 2. The QE curve for the devices corresponding to component cells in the triple cell structure along with a highly Ge rich sample is shown in Fig. 3.

The stability test under the prolonged light soaking (1000 h) under AM1 light from a halogen lamp was also performed to study the degradation of these devices. The I–V performance was measured at different stages of light soaking. Both FF and η decrease as exposure time increases. However, when exposure time increased beyond 100 h, a nearly saturated state is reached. A good reproducibility between the samples, prepared under identical condition (such as GD435 and GD443) is observed. Table 2 lists the percentage decrease η after 1000 h of light soaking. We observe that our top cell shows least degradation (2–4%), whereas the degradation is more as [Ge] increases. The cells with very high concentration of germanium show less degradation, but there starting FF and η is also low. The germanium rich cells show higher degradation then our standard triple junction solar cells, because in the single junction structure, these receive much more light then when in a stack of three cells in the triple junction solar cells.

In another important measurements, we measured the subgap QE for these solar cells and

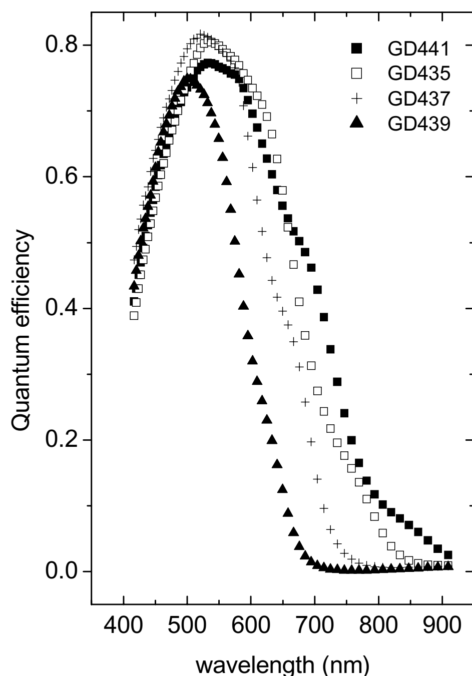

Fig. 3. QE curves for the series of a-SiGe:H n–i–p solar cells with different Ge content corresponding to bottom (GD435), middle (GD437) and top (GD439) cells in our triple junction solar cell structure including a highly Ge rich cell (GD441). The error is included in the symbol size.

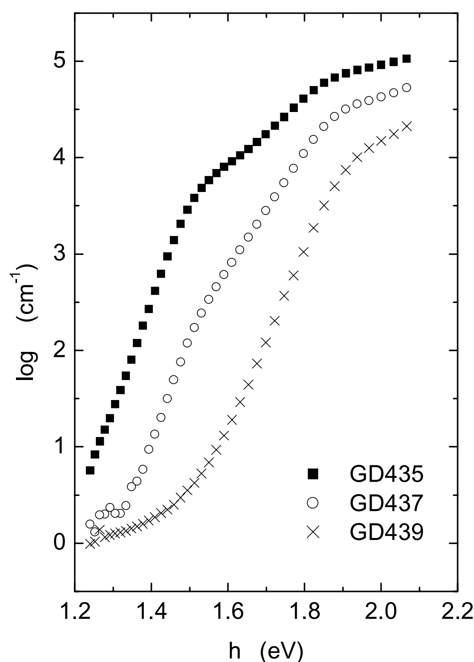

Fig. 4. $\log\alpha$ vs. $h\nu$ (as determined by subgap QE measurements) for a-SiGe:H n–i–p solar cells with different Ge content. The error is included in the symbol size.

knowing the thickness of the i-layer in the device, calculated the absorption coefficient α as a function of energy [8]. Fig. 4 shows the $\log\alpha$ vs. $h\nu$ for cells corresponding to top, mid and bottom cells. The band gap E_g is calculated where $\alpha = 2000\ \text{cm}^{-1}$. The Urbach tail slope (E_0) in the region below E_g is calculated using $\alpha = \alpha_0 \exp(E/E_0)$ and the values of E_g and E_0 are listed in Table 2. It is observed that E_g thus obtained matches quite well with that obtained for single layer using transmission measurements. It gives us the confidence that the material properties are not changed in the device structure.

4. Conclusions

We have presented our results for a-SiGe single layers and corresponding n–i–p devices with $[GeH_4]/[Si_2H_6]$ ratio varying from 1.43 to 0. As the Ge content increases in these films, less hydrogen is incorporated in the films. Further, a part of the hydrogen goes in to Ge–H mode as well. The ratio of hydrogen in dihydride to monohydride mode also increases with increasing Ge content, except for highly Ge rich films, where it is low, but in these films, the hydrogen also goes in to Ge–H_2 mode as well.

n–i–p devices made using these i-layers show that as Ge content increases, V_{oc} decreases, J_{sc} increases along with a decrease in FF and efficiency. Also, the Ge rich films degrade more under prolonged exposure to light, except for highly Ge rich devices, however, there starting FF and η is also low, making them useless for devices. Our studies show that so far the composition used our present triple junction recipe seems to be the best, however, a slight modification in Ge content or hydrogen content may be useful in improving the device performance. The estimation of band gap and Urbach tail slope using QE measurements in subgap absorption measurements show that the material properties do not change in the device

and the technique can be used for the estimation of absorber layer parameters in the device.

Acknowledgements

The work reported here is supported by NREL under Thin Film partnership program (No. ZAF-8-17619-14).

References

[1] J. Yang, A. Banerjee, S. Sugiyama, S.Guha, in: Proceedings of 2nd World Conference on Photovoltaic Solar Energy Conversion, Vienna, Austria, July 1998.
[2] X. Deng, X. Liao, S. Han, H. Povolny, P. Agarwal, Sol. Energy Mater. Sol. Cells 62 (2000) 89.
[3] R. Swanpole, J. Phys. E 16 (1983) 1214.
[4] C.J. Fang, K.J. Gruntz, L. Ley, M. Cardona, F.J. Demond, G. Muller, S. Kalbitzer, J. Non-Cryst. Solids 35&36 (1980) 255.
[5] X.B. Liao, J. Walker, X. Deng, Mater. Res. Soc. Symp. Proc. 557 (1999) 779.
[6] T. Shimizu, M. Kumeda, A. Morimoto, Y. Tsujimura, L. Kobayashi, Mater. Res. Soc. Sym. Proc. 70 (1986) 313.
[7] S.S. Hedegus, R.E. Rocheleau, R.M. Tullman, D.E. Albright, N. Saxena, W.A. Buchanan, K.E. Schubert, R. Dozier, in: Proceedings of the 20th IEEE PV Specialists Conference, 1988, p. 129.
[8] T.X. Zhou, S.S. Hedegus, C.M. Fortman, Mater. Res. Soc. Symp. Proc. 219 (1991) 45.